Available online at www.sciencedirect.com
ScienceDirect
Chinese Journal of Aeronautics 23(2010) 438-446
Chinese Journal of Aeronautics
www.elsevier.com/locate/cja

Enhanced GPS Measurements Simulation for Space-oriented Navigation System Design

Wang Liduan[a,*], Zhai Chuanrun[b], Jin Wenrui[c], Zhan Xingqun[b]

[a]*School of Electronic, Information and Electrical Engineering, Shanghai Jiao Tong University, Shanghai 200240, China*

[b]*School of Aeronautics and Astronautics, Shanghai Jiao Tong University, Shanghai 200240, China*

[c]*Sino-German College of Applied Sciences, Tongji University, Shanghai 201804, China*

Received 14 September 2009; accepted 4 March 2010

Abstract

At the stage of preliminary scheme and algorithm design for spaceborne navigation systems, a precise and high-fidelity software global positioning system (GPS) simulator is a necessary and feasible testing facility in laboratory environments, with consideration of the tradeoffs where possible. This article presents a software GPS measurements simulator on the L1 C/A code and carrier signal for space-oriented navigation system design. The simulator, coded in MATLAB language, generates both C/A code pseudorange and carrier phase measurements. Mathematical models in the Earth centered inertial (ECI) frame are formulated to simulate the GPS constellation and to generate GPS measurements. A series of efficient measures are investigated and utilized to rationalize the enhanced simulator, in terms of ephemeris data selection, space ionospheric model and range rate calculation, etc. Such an enhanced simulator has been facilitating our current work for designing a space integrated GPS/inertial navigation system (INS) navigation system. Consequently, it will promote our future research on space-oriented navigation system.

Keywords: global positioning system; pseudorange; carrier phase; measurements simulator; space applications; navigation systems

1. Introduction

Global positioning system (GPS) has made a great success in spacecraft navigation since the mid 1990s[1-2], while more challenges were encountered along with diverse requirements of new applications. GPS is susceptible to interference, multipath, blockage, or other outage sources. In that case, the GPS-only navigation system is not reliable or totally sufficient to meet the requirements deriving from different spaceflight phases. At the same time, the development of inertial navigation system (INS) with new inertial sensors has advanced its applications to space flight. In recent years, GPS/INS integration has become one preferable solution to spacecraft navigation, which could overcome the weaknesses[3] of GPS and INS, and assure availability and continuity of navigation information.

The applications and rapid evolution of space-oriented GPS or integrated GPS/INS navigation system demand the most current testing and verification means. Instead of hardware-in-the-loop test facilities and flight tests, simulation is a first reasonable step of evaluating the newly developed algorithms of space-oriented navigation system. To generate diverse scenarios and measurement data for the simulation process, numerous GPS simulators have been developed on the basis of software-only[3] or hybrid architecture integrated with hardware[4-6]. Hybrid GPS simulator is also named as global navigation satellite system (GNSS) testing and verification system. The hybrid simulator provides a superior navigation and positioning testing and verification solutions to the software-only GPS simulator. Nevertheless many researchers and groups cannot afford its high price. Considering tradeoff between cost and performance, software GPS simulator is a most feasible means to evaluate GPS related algorithms and system in laboratory environment. However, most of software GPS simulators (or GPS simulation toolboxes) are dedicated to assisting the design of terrestrial, airborne and nautical navigation systems.

Different from those former fields, space vehicles generally travel through or in the ionosphere at high

*Corresponding author. Tel.: +86-21-34205622.
E-mail address: lidwang@gmail.com
Foundation item: Research Fund of Shanghai Academy of Spaceflight Technology

doi: 10.1016/S1000-9361(09)60239-9

speed. In terms of space application environments, a software GPS measurements simulator is proposed in the article, which directly serves to space-oriented navigation system design. A series of measures are employed to achieve enhanced performance, such as high precision and fidelity. First of all, for a given simulation progress, the ephemeris data term whose time is closest to the simulation time would be picked out from the ephemeris data file. Second, the simulated GPS measurements cover all necessary errors, such as range rate contributions, satellite clock correction, receiver clock error, ionospheric delay, ephemeris and satellite clock residual errors, etc. And we have attempted to analyze the effects of weight of the errors on different simulated space scenarios and the GPS satellites visibility. Moreover, an ionospheric model for GPS tracking of low Earth orbit (LEO) satellites proposed by O. Montenbruck, et al.[7], is introduced into the simulator. In addition, to achieve creditable pseudorange measurement of space environments, the range rate incurred by the high speed of space GPS receiver is considered[8]. Formulae of the range rate for space applications are also specified.

In this study, GPS simulation is driven by the true trajectories of space vehicles. That is, GPS (and INS) measurements are derived from the trajectories. Accordingly, the qualitative performance and feasibility of proposed GPS/INS integration system are evaluated with those simulated measurements. The interaction diagram between GPS simulator and space-oriented integrated navigation system is depicted in Fig.1.

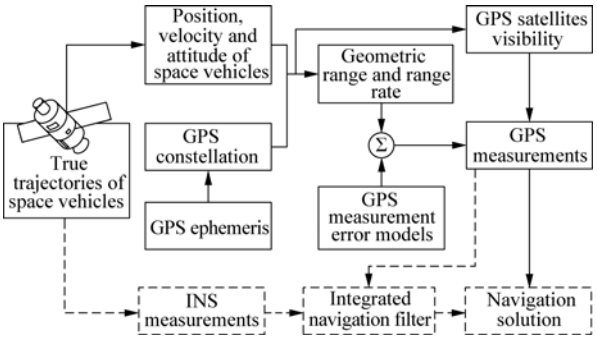

Fig.1 Interaction between GPS simulator and space-oriented navigation system.

Space vehicles (SVs) in Fig.1 and the following sections represent the spacecraft for which we develop navigation system, such as various satellites, space shuttles or space transportation vehicles, etc. Correspondingly, we use GPS satellites denoting the space vehicles of GPS constellation. The rest of this article provides the processes of generating the space-oriented GPS measurements in detail.

2. Simulation Overview

Fig.2 presents an overview of the GPS simulator. The

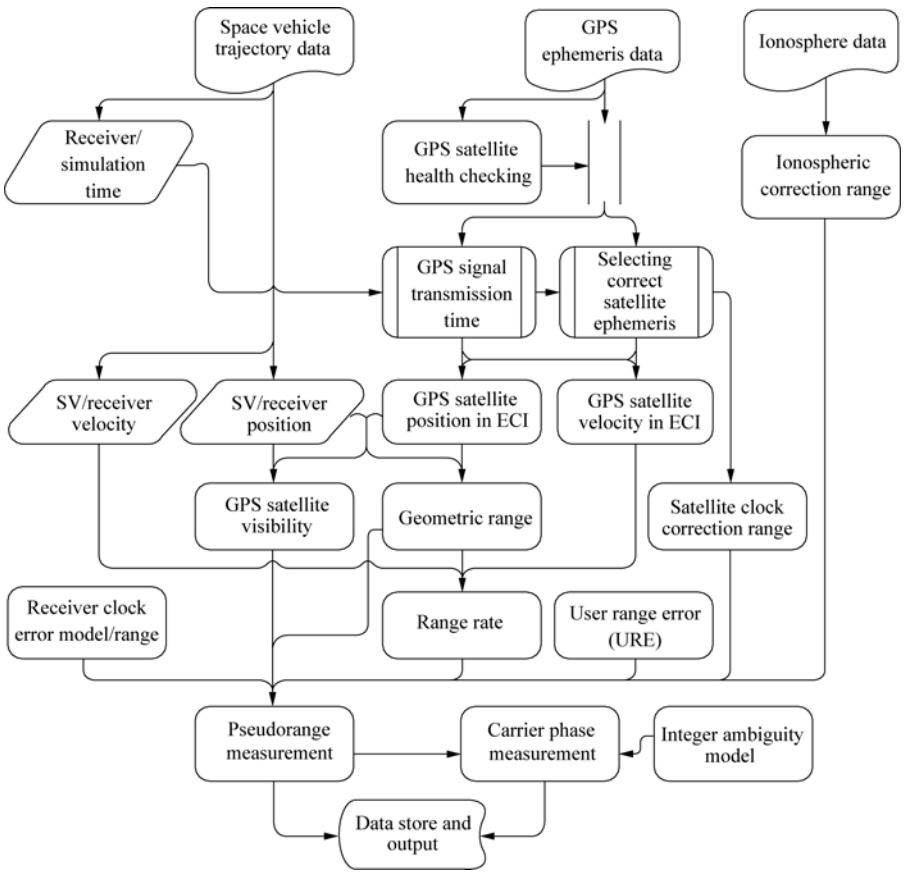

Fig.2 Space-oriented GPS measurements generation diagram.

configuration of GPS measurements comprises the following elements and modules.

Reference frame: Different from the local geographic frame and the Earth-centered Earth-fixed (ECEF) frame for the navigation computations in most terrestrial and aeronautical applications, the Earth centered inertial (ECI) frame is the prior space-oriented navigation frame and selected as the reference frame of the GPS simulator.

Simulation time: Simulation time is usually given by coordinated universal time (UTC), which is related to GPS time (GPST), i.e. GPS system time. It is feasible to take only GPST as a uniform time scale in the GPS simulator. Instead of GPS week number and seconds of the week, modified Julian date (MJD) time format is used to express GPST for more convenient simulation[3].

GPS satellite health checking: The program gets rid of the ephemerides from sick GPS satellites.

GPS signal transmission time: Caring for GPS satellite motion during signal propagation, an iterative scheme is used to figure out signal transmission time in this module.

Ephemeris selection: The module picks out the ephemeris data term from ephemeris data file with the time most recent to simulation time.

GPS constellation: For space-oriented navigation system design, GPS satellite position and velocity are solved to simulate GPS constellation in the ECI frame. More details on GPS constellation are provided in the next section.

Geometric range: Geometric range is the true distance from GPS satellite to the user receiver (i.e. spacecraft) in the ECI frame. And it is the function of transmission and reception time. Given signal propagation time Δt, geometric range is computed by multiplying Δt by the speed of light.

GPS satellite visibility: The module works out the number of GPS satellites in view at all simulation time for spacecraft-carried receiver. The satellite visibility is mainly decided by the receiver antenna direction and Earth shadow, which will be discussed later.

Range rate: According to T. Ebinuma[8], the range rate contributes over 6 m to pseudorange measurement for a GPS receiver operating in a low Earth orbit, on condition that the receiver clock bias is less than 1 ms. Therefore, the contribution should be taken into account for pseudorange measurement generation of the space-oriented GPS simulator, as well as for carrier phase measurement simulation.

GPS satellite clock correction: Generally, the user is allowed to correct the code phase offset of GPS satellite pseudo-random noise (PRN) making use of the polynomial coefficients in the ephemeris data[9]. On the contrary, the correction could be added to the simulated GPS measurements, establishing a high-fidelity scenario.

Receiver clock error: In the module, a receiver clock model, including the clock bias and drift errors, is necessary to simulate contributions of the clock error to GPS measurements.

Ionospheric and tropospheric delay errors: Ionospheric delay for space-oriented single frequency measurements is different from that of other GPS positioning applications on the Earth surface. Based on O. Montenbruck's research[7] about ionospheric correction for LEO satellites navigation, a corresponding delay model is introduced into GPS measurement simulation. The ionospheric modeling error is incorporated into user range error (URE). Tropospheric delay is excluded from the measurements because the SVs or spacecraft are assumed to operate above the troposphere.

Multipath: It is difficult to set up a universal and practical multipath model for most of spacecraft, since the multipath signals are reflected by various surfaces, and also affected by SVs' motion relative to GPS satellites. A statistical multipath model was selected in place of a geometrical model by D. E. Gaylor[3]. However, it is only effective for some specific SVs. Hence, we would ignore the error attributed to multipath in the measurements. There is also a simple way to simulate the range error due to multipath as random noise with a 1 m-standard deviation, since the error is quasi-sinusoidal and could be thought as noise[10].

User range error: The ephemeris and GPS satellite clock uncorrected (or, residual) errors change slowly, like the ionospheric modeling error. Both of them would be classified as biases by P. Misra and P. Enge[10]. The combination of these three kinds of errors is referred to as the URE.

Pseudorange measurement: In view of the error sources and models discussed formerly, pseudorange measurement is generated by this module.

Integer ambiguity: The model calculates the integer ambiguity, which is regarded as a bias error associated with each carrier phase measurement.

Carrier phase measurement: Carrier phase measurement is derived from pseudorange measurement and integer ambiguity.

3. GPS Constellation Model

The mathematical formulation of GPS satellite position in the ECI frame is slightly different from the algorithms in the ECEF frame specified in Ref.[9]. In the following sections, we use I and O to denote the ECI frame and the orbit plane frame respectively. The GPS satellite position vector in the orbit plane can be expressed as

$$\boldsymbol{r}_{\mathrm{O}} = \begin{bmatrix} r\cos u \\ r\sin u \\ 0 \end{bmatrix} \tag{1}$$

where r is the corrected radius, u the corrected argument of latitude, both of which are computed using ephemeris parameters.

In disregard of the Earth rotation in the ECI frame, the corrected longitude of ascending node is given by

$$\Omega = \Omega_0 + \Delta t\dot{\Omega} \tag{2}$$

where Ω_0 is the longitude of ascending node of orbit plane at weekly epoch, $\dot{\Omega}$ the rate of right ascension and Δt the escaped time from the ephemeris reference epoch to the GPS system time of transmission.

Rotating the position vector $\boldsymbol{r}_{\mathrm{O}}$ to the ECI frame, we obtain the desired position

$$\boldsymbol{r}_{\mathrm{ECI}} = \boldsymbol{R}_{\mathrm{O}}^{\mathrm{I}}\boldsymbol{r}_{\mathrm{O}} = \boldsymbol{R}_z(-\Omega)\boldsymbol{R}_x(-i)\boldsymbol{r}_{\mathrm{O}} \tag{3}$$

where $\boldsymbol{R}_z$ and $\boldsymbol{R}_x$ are rotation matrixes about the third axis and first axis through an angle of $-\Omega$ and $-i$ respectively, i is the corrected inclination angle, $\boldsymbol{R}_{\mathrm{O}}^{\mathrm{I}}$ is the coordinate transformation matrix from the orbit plane frame to the ECI frame, so

$$\boldsymbol{R}_{\mathrm{O}}^{\mathrm{I}} = \begin{bmatrix} \cos\Omega & -\sin\Omega\cos i & \sin\Omega\sin i \\ \sin\Omega & \cos\Omega\cos i & -\cos\Omega\sin i \\ 0 & \sin i & \cos i \end{bmatrix} \tag{4}$$

Taking the first derivative of Eq.(3) relative to time, the ECI velocity of GPS satellite can be expressed as

$$\boldsymbol{v}_{\mathrm{ECI}} = \dot{\boldsymbol{R}}_{\mathrm{O}}^{\mathrm{I}}(\Omega,i)\boldsymbol{r}_{\mathrm{O}} + \boldsymbol{R}_{\mathrm{O}}^{\mathrm{I}}(\Omega,i)\dot{\boldsymbol{r}}_{\mathrm{O}} \tag{5}$$

The velocity vector in the orbit frame is the time derivative of the orbit frame position given in Eq.(1), it can be expressed as

$$\dot{\boldsymbol{r}}_{\mathrm{O}} = \begin{bmatrix} \dot{r}\cos u - r\dot{u}\sin u \\ \dot{r}\sin u + r\dot{u}\cos u \\ 0 \end{bmatrix} \tag{6}$$

where $\dot{r}$ and $\dot{u}$ are the time derivatives of the corrected radius and argument of latitude respectively.

The first derivative of the rotation matrix $\dot{\boldsymbol{R}}_{\mathrm{O}}^{\mathrm{I}}$ relative to time is given by

$$\dot{\boldsymbol{R}}_{\mathrm{O}}^{\mathrm{I}} = \dot{\Omega}\begin{bmatrix} -\sin\Omega & -\cos\Omega\cos i & \cos\Omega\sin i \\ \cos\Omega & -\sin\Omega\cos i & \sin\Omega\sin i \\ 0 & 0 & 0 \end{bmatrix} + \left(\psi + \delta\dot{i}\right)\begin{bmatrix} 0 & \sin\Omega\sin i & \sin\Omega\cos i \\ 0 & -\cos\Omega\sin i & -\cos\Omega\cos i \\ 0 & \cos i & -\sin i \end{bmatrix} \tag{7}$$

where ψ is the rate of inclination angle from the broadcast ephemeris, and $\delta\dot{i}$ the time derivative of inclination correction.

4. GPS Measurements for Space Applications

4.1. Measurement models

Both pseudorange and carrier phase measurements are formulated in this section. Firstly, let us denote by t_{S} the reading of the satellite clock at transmission time and by t_{R} the reading of the receiver clock at GPS signal time. The delays of the clocks with respect to GPS system time are termed δt_{R} and δt_{S}. Thus, the measured pseudorange is defined as

$$P(t_{\mathrm{R}}) = c(t_{\mathrm{R,GPST}} - t_{\mathrm{S,GPST}}) + c(\delta t_{\mathrm{R}} - \delta t_{\mathrm{S}}) = \rho(t_{\mathrm{R,GPST}}) + c(\delta t_{\mathrm{R}} - \delta t_{\mathrm{S}}) \tag{8}$$

where c is the speed of light, and $\rho(t_{\mathrm{R,GPST}})$ the geometric range between the receiver position at reception time $t_{\mathrm{R,GPST}}$ and the satellite position at transmission time $t_{\mathrm{S,GPST}}$. Both of the time epochs are expressed in GPS system time.

The reading of the receiver clock t_{R} is provided; yet the true receiver time $t_{\mathrm{R,GPST}}$ (or the GPS system time) is unknown. The geometric range is often expanded into a Taylor series around the known receiver measured time[8]

$$\rho(t_{\mathrm{R,GPST}}) \approx \rho(t_{\mathrm{R}}) - \dot{\rho}(t_{\mathrm{R}})\delta t_{\mathrm{R}} \tag{9}$$

The geometric range $\rho(t_{\mathrm{R}})$ is the modulus of the line of sight vector, which is computed by

$$\rho(t_{\mathrm{R}}) = \left|\boldsymbol{r}_{\mathrm{R}}(t_{\mathrm{R}}) - \boldsymbol{r}_{\mathrm{S}}(t_{\mathrm{S}})\right| \tag{10}$$

where $\boldsymbol{r}_{\mathrm{R}}(t_{\mathrm{R}})$ and $\boldsymbol{r}_{\mathrm{S}}(t_{\mathrm{S}})$ are the position vectors of the receiver and GPS satellite respectively. The instantaneous range rate $\dot{\rho}(t_{\mathrm{R}})$ [8] is expressed as

$$\dot{\rho}(t_{\mathrm{R}}) = \frac{(\boldsymbol{r}_{\mathrm{R}}(t_{\mathrm{R}}) - \boldsymbol{r}_{\mathrm{S}}(t_{\mathrm{S}}))\cdot(\dot{\boldsymbol{r}}_{\mathrm{R}}(t_{\mathrm{R}}) - \dot{\boldsymbol{r}}_{\mathrm{S}}(t_{\mathrm{S}}))}{\rho(t_{\mathrm{R}}) - (\boldsymbol{r}_{\mathrm{R}}(t_{\mathrm{R}}) - \boldsymbol{r}_{\mathrm{S}}(t_{\mathrm{S}}))\cdot(\dot{\boldsymbol{r}}_{\mathrm{S}}(t_{\mathrm{S}})/c)} \tag{11}$$

where "·" denotes the inner product of two vectors. And the instantaneous range rate of the jth GPS satellite can be expressed as

$$\dot{\rho}_j(t_{\mathrm{R}}) = \frac{\boldsymbol{\rho}_j \cdot \boldsymbol{v}_{\mathrm{REL}j}}{\rho_j(t_{\mathrm{R}}) + \boldsymbol{\rho}_j \cdot (\boldsymbol{v}_{\mathrm{S}j}(t_{\mathrm{S}})/c)} \tag{12}$$

where $\boldsymbol{\rho}_j$ is the line of sight vector from the receiver to the jth GPS satellite, $\boldsymbol{v}_{\mathrm{REL}j}$ the relative velocity between them, and $\boldsymbol{v}_{\mathrm{S}j}(t_{\mathrm{S}})$ the velocity of the jth GPS satellite. More details on the formulae of range rate are provided in Appendix A.

Accounting for various error sources related to code phase measurement such as the receiver and GPS satellite clock errors, ionospheric delay, URE, unmodeled effects and measurement error etc., the pseudorange measurement can be written as

$$P(t) = \rho - \dot{\rho}\delta t_{\mathrm{R}} + c(\delta t_{\mathrm{R}} - \delta t_{\mathrm{S}}) + \Delta\rho_{\mathrm{iono}} + \Delta\rho_{\mathrm{URE}} + \varepsilon \tag{13}$$

where $\Delta\rho_{\mathrm{iono}}$ is ionospheric delay error, $\Delta\rho_{\mathrm{URE}}$ is user range error and ε represents unmodeled effects, modeling error and measurement error[10]. As mentioned formerly, multipath effects and tropospheric delay are left out of consideration for space-oriented GPS measurement generation. For other application environments, a specific but practical multipath error model is indispensable to an accurate simulation.

Multiplied the carrier phase Φ expressed in cycles by

the wavelength λ, it can be scaled to a range which only differs from the code pseudorange by the integer ambiguity N multiples of λ. By virtue of the pseudorange measurement given in Eq.(13), it is easy to formulate carrier phase measurement equation by

$$\lambda\Phi = \rho - \dot{\rho}\delta t_{\mathrm{R}} + c(\delta t_{\mathrm{R}} - \delta t_{\mathrm{S}}) + \Delta\rho_{\mathrm{iono}} + \Delta\rho_{\mathrm{URE}} + \lambda N + \varepsilon \quad (14)$$

where the integer ambiguity N for each carrier measurement can be modeled as a zero-mean, Gaussian random variable with a standard deviation of 1×10^6 cycles[3].

4.2. Receiver clock model

The receiver clock model is described by P. Axelrad and R. G. Brown[11]. Two required states, i.e. the receiver clock bias and drift, which represent the phase and frequency errors of the receiver crystal oscillator, are estimated. Both the frequency and phase are expected as random walk over a short period of time. Considering the space vehicles travelling in high speed in orbit (refer to Ref.[8]), the discrete process equations are expressed as follows:

$$\boldsymbol{b}(t_{k+1}) = \boldsymbol{\Phi}_{\mathrm{b}}(t_k, t_{k+1})\boldsymbol{b}(t_k) + \boldsymbol{w}_{\mathrm{b}}(t_k) + c\boldsymbol{h}_{\mathrm{b}} \quad (15)$$

where

$$\boldsymbol{b} = \begin{bmatrix} b \\ f \end{bmatrix},\ \boldsymbol{\Phi}_{\mathrm{b}}(t_k, t_{k+1}) = \begin{bmatrix} 1 & \Delta T \\ 0 & 1 \end{bmatrix},\ \boldsymbol{h}_{\mathrm{b}} = \begin{bmatrix} h_b\Delta T \\ 0 \end{bmatrix}$$

$\boldsymbol{w}_b$ is the clock noise, b the receiver clock bias, f the clock drift, and h_b the relativistic effect term. In near circular orbits around the Earth, h_b can be approximated as a constant, defined as

$$h_{\mathrm{b}} = \frac{1}{c^2}\left(\frac{\mu}{R_{\mathrm{E}}} - \frac{\mu}{\overline{R}} - \frac{\overline{V}^2}{2}\right)$$

where μ is the Earth's gravitational constant defined by WGS-84, R_{E} the mean equatorial radius of the Earth, $\overline{R}$ the average distance of the receiver from the center of the Earth, and $\overline{V}$ the average velocity of spacecraft in the ECI frame[8].

The process noise covariance matrix of the receiver clock state vector $\boldsymbol{b}$ is

$$\boldsymbol{Q}_{\mathrm{b}} = E\{\boldsymbol{w}_{\mathrm{b}}\boldsymbol{w}_{\mathrm{b}}^{\mathrm{T}}\} = \begin{bmatrix} S_{\mathrm{f}}\Delta T + S_{\mathrm{g}}\dfrac{\Delta T^3}{3} & S_{\mathrm{g}}\dfrac{\Delta T^2}{2} \\ S_{\mathrm{g}}\dfrac{\Delta T^2}{2} & S_{\mathrm{g}}\Delta T \end{bmatrix}$$

where the process (or, white) noise power spectral amplitudes S_{f} and S_{g} can be related to the Allan variance parameters, whose quantities vary widely depending on the receiver crystal oscillator. Typical values for temperature controlled crystal oscillators commonly used on commercial GPS receivers are [12]

$$S_{\mathrm{f}} = 1.0c^2\times10^{-19}\ \mathrm{m^2/s}$$
$$S_{\mathrm{g}} = 4.0c^2\pi^2\times10^{-20}\ \mathrm{m^2/s^3}$$

4.3. Ionospheric model for spaceborne receiver

A well-known empirical ionospheric model, named as Klobuchar model in honor of its developer Klobuchar, was adopted by the GPS control segment (CS), whose parameter values are broadcast by the GPS satellites. The model represents the zenith delay as a constant value at nighttime and a half-cosine function in daytime[10]. But then, the Klobuchar model is defined for users below the ionospheric top layer, which is not suitable for a spaceborne receiver. As for this study, we make use of an improved ionospheric model for LEO spaceborne receiver proposed by O. Montenbruck, et al.[7] to generate ionospheric delay error.

With the Montenbruck's model, the ionospheric path delay for positive elevations is obtained from thin layer approximation with a suitably chosen effective height above the receiver. The pseudorange measurements taken at L_1 frequency f_{L_1} experience a group delay

$$\Delta\rho_{\mathrm{iono}} = \alpha M(E_{\mathrm{IP}})\mathrm{TEC}(\lambda_{\mathrm{IP}}, \varphi_{\mathrm{IP}}, 0)\frac{40.3\ \mathrm{m^3\cdot s^{-2}}}{f_{\mathrm{L_1}}^2} \quad (16)$$

where the scale factor α, the mapping function $M(E_{\mathrm{IP}})$ and the total electron content $\mathrm{TEC}(\lambda_{\mathrm{IP}},\varphi_{\mathrm{IP}},0)$ of the ionosphere on the ground at geographical coordinates $(\lambda_{\mathrm{IP}},\varphi_{\mathrm{IP}})$ will be discussed subsequently.

Inasmuch as the path length in the ionosphere increases with the decreasing elevation, the mapping function $M(E_{\mathrm{IP}})$ is given by

$$M(E_{\mathrm{IP}}) = \frac{1}{\sin(E_{\mathrm{IP}})} = \left\{1 - \left[\cos(E_{\mathrm{R}})\frac{\boldsymbol{r}_{\mathrm{R}}}{\boldsymbol{r}_{\mathrm{IP}}}\right]^2\right\}^{-1/2} \quad (17)$$

where E_{R} is the positive elevation of spaceborne receiver at the position $\boldsymbol{r}_{\mathrm{R}}$, and E_{IP} the elevation ($E_{\mathrm{IP}} \geq E_{\mathrm{R}}$) at the ionospheric point $\boldsymbol{r}_{\mathrm{IP}}$.

The scale factor α relates the total electron content $\mathrm{TEC}(\lambda_{\mathrm{IP}},\varphi_{\mathrm{IP}},h_{\mathrm{IP}})$ of the ionosphere above altitude h_{IP} to the total electron content (TEC) above ground at geographical coordinates $(\lambda_{\mathrm{IP}},\varphi_{\mathrm{IP}})$, which is formulated as

$$\alpha = \frac{e - \exp\{1 - \exp[-(h_{\mathrm{IP}} - h_0)/H]\}}{e - \exp[1 - \exp(h_0/H)]} \quad (18)$$

where e is the mathematical constant, the adjusted inflection point altitude h_0 = 420 km and scale height H = 100 km, assuming a Chapman profile describes the altitude variation of the electron density. The global surface TEC maps are obtained from the international GPS service (IGS) network. Although the model is developed for LEO spacecraft, it is still competence for the spaceborne receiver with higher orbits and operat-

ing within the ionosphere. However, there is one worthy of attention: the discussion on the Montenbruck's model is under the provision that the elevation for ionospheric path delay is positive.

Furthermore, the receiver with an altitude over the ionosphere is still influenced by the ionosphere because it can see GPS satellites through the ionosphere. Fairly precise but complicated ionospheric models are deeply analyzed by P. Gustavsson[13]. Likewise, some others regional models could be utilized for more accurate simulation of ionospheric delay. On the contrary, the Montenbruck's model can be used to correct the ionospheric delay of spaceborne GPS receivers, in view of its original function. Two general ionospheric path delay models are briefly summarized in Ref.[14] for orbiting spacecraft. The models are relevant to hard-and software- simulations as well as measurement correction in single frequency GPS receivers. It is obvious that each model presented above has its own constraints for different applications. Consequently, the sound selection of ionospheric models must be well application-dependent.

4.4. User range error

The 3D ephemeris error over a day is typically 3-5 m root mean square (RMS)[10]. According to the Ref.[15], we select the three-axis standard deviations of ephemeris error respectively

$$\boldsymbol{\sigma}_{\text{eph}} = \begin{bmatrix} \sigma_{\text{radial}} \\ \sigma_{\text{cross-track}} \\ \sigma_{\text{along-track}} \end{bmatrix} = \begin{bmatrix} 0.8 \\ 2.5 \\ 3.6 \end{bmatrix} \text{ m}$$

Therefore, the 3D standard deviation used in our simulation is 4.5 m RMS. The effective pseudorange and carrier phase errors due to ephemeris prediction errors can be computed by projecting the satellite position error vector onto the satellite-to-user line of sight (LOS) vector. The effective pseudorange measurement error $\Delta\rho_{\text{eph}}$ due to the ephemeris error is formulated as[3]

$$\Delta\rho_{\text{eph}} = \frac{\boldsymbol{\varepsilon}_{\text{eph}}^{\text{ECI}} \bullet \boldsymbol{\rho}_j}{\rho_j} \tag{19}$$

where $\boldsymbol{\varepsilon}_{\text{eph}}^{\text{ECI}}$ is the ephemeris error vector in the ECI frame and $\boldsymbol{\rho}_j/\rho_j$ is the LOS unit vector of the receiver to the jth GPS satellite. In this way, the effective pseudorange or carrier phase error $\Delta\rho_{\text{eph}}$ is on the order of 0.8 m (1σ)[16].

The residual clock error depends on the type of satellite and age of the broadcast data. In accordance with the data presented by J. Taylor, et al.[17], the nominal σ clock error $\Delta\rho_{\text{S,resi}}$ for the GPS constellation in 2004 averaged over age of data (AOD) is 1.1 m, that is, the standard deviation σ_{St} of the residual clock error.

The effective accuracy of the ionospheric modeling is about 2-5 m in ranging for users in the temperate zones[18]. The ionospheric modeling error $\delta\rho_{\text{iono}}$ is assumed 4 m (the standard deviation σ_{iono}=4 m) for the ionospheric simulation.

As hinted earlier, the ephemeris, satellite residual clock errors and the ionospheric modeling error are all thought as measurement bias. The combined errors URE accounting for these three kinds of error sources would be modeled as the exponentially correlated random variable (ECRV) for each GPS satellite[8], with the standard deviations $\boldsymbol{\sigma}_{\text{eph}}$, σ_{St} and σ_{iono} respectively. The URE, denoted as $\Delta\rho_{\text{URE}}$, is directly described as

$$\Delta\rho_{\text{URE}} = \Delta\rho_{\text{eph}} + \Delta\rho_{\text{S,resi}} + \delta\rho_{\text{iono}} \tag{20}$$

5. GPS Satellites Visibility

The number of satellites in view is one of important characteristics of GPS satellite constellation as they relate to user receiver navigation performance[19]. It is critical for GPS-only positioning that at least four satellites should be in view, but it is highly desirable that five or more should be in view at all times.

The GPS satellite visibility by a spaceborne receiver mainly depends on three factors, namely the Earth shadow, the direction the receiver antenna points to, and the receiver position or altitude. A simple visibility model for spaceborne receivers is illustrated in Fig.3. Given that receiver antenna is pointed along the receiver position vector, the GPS satellite would be in view, if only the declination angle θ_j between the antenna boresight and the LOS vector is smaller than the complementary angle of elevation mask angle α.

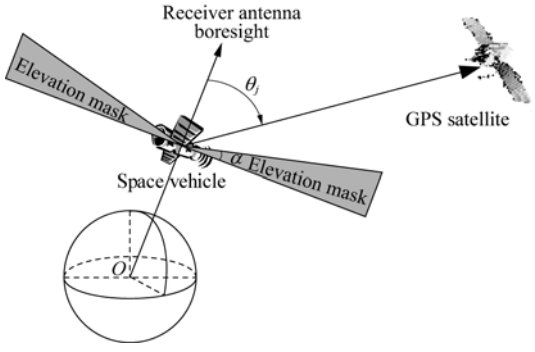

Fig.3 GPS satellite visibility model for spaceborne receiver.

The satellite visibility for the Earth surface region with a 5° elevation mask angle in common use is presented in Ref.[19]. However, a moderately high altitude space vehicle can view satellites down to 0° elevation angle, and even has better satellite visibility. Fig.4 demonstrates GPS constellation status and satellites visibility at the 500th second of simulation time. In Fig.4, PRN 15 outage indicates the PRN number 15 does not exist in the ephemeris data of measurements simulation. And the sick status of PRN 32 means its

navigation data are bad. Thus, both PRN 15 and PRN 32 are excluded from GPS constellation in the whole simulation process. Also presented in Fig.4 is the visibility of the left 30 GPS satellites at the simulation epoch. The simulation result of GPS satellites visibility over the entire simulation time from MJD 54 240 to 54 240.999 8 is shown in Fig.5. A 0° and a 5° positive elevation mask angles are used for comparison.

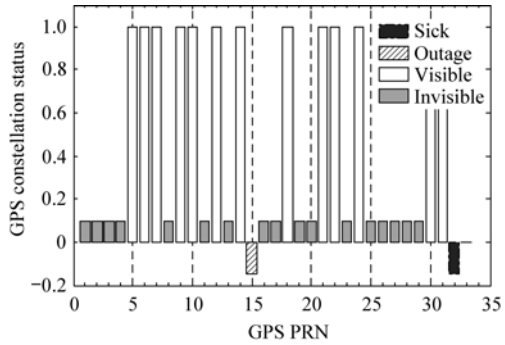

Fig.4 GPS constellation status and visibility at the 500th second of simulation time.

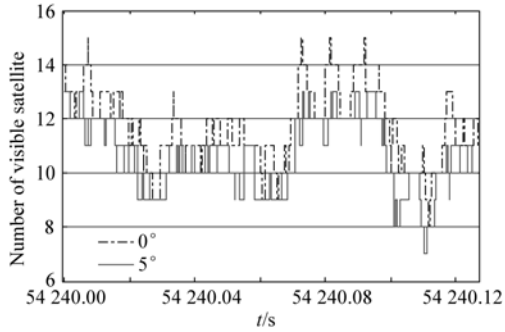

Fig.5 Number of visible GPS satellites as space vehicle operates in orbits.

The result shows that at least 7 GPS satellites are in view at all times for the 5° elevation mask angle, and for most of the time at least 9 satellites are in view. There is a minimum of 8 satellites visible for the 0° elevation mask angle. In a word, space-oriented navigation environments have far better visibility than that of ground use, though we neglect negative elevation mask angles here.

6. Simulation Results

The total simulation time lasts 10 960 s, and the broadcast ephemeris data on May 20, 2007 from IGS are adopted in the article. That is to say, the space-oriented GPS simulator is performed from the [1 428, 0] to [1 428, 86 384] in GPST ([week number, seconds of the week]), i.e. from MJD 54 240 to 54 240.999 8.

The GPS measurement simulation is driven by the true trajectory of a space vehicle, as shown in Fig.6. Fig.7 demonstrates the GPS constellation over the entire simulation time.

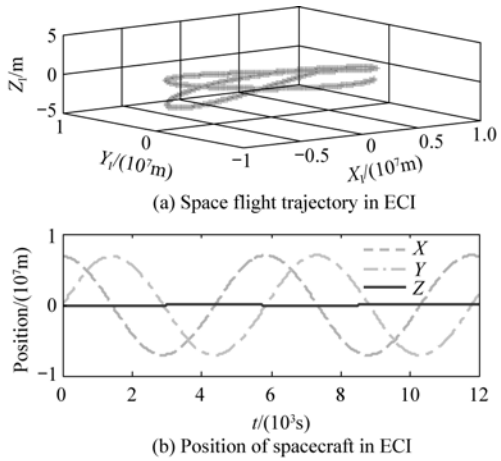

Fig.6 True trajectory of space vehicle.

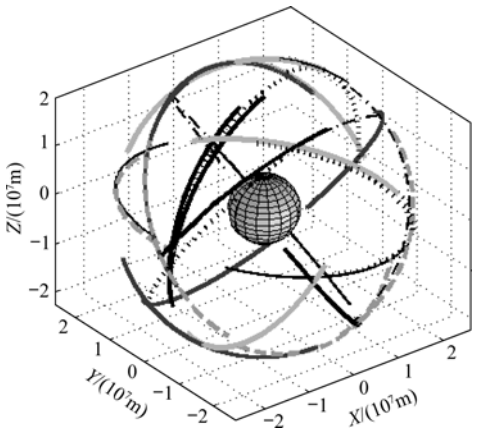

Fig.7 GPS constellation in ECI frame (30 GPS satellites).

As the GPS satellites are visible, the geometric ranges between the space vehicle and 30 GPS satellites are calculated and shown in Fig.8.

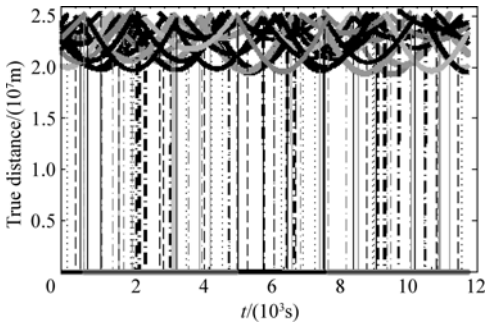

Fig.8 Geometric ranges between space vehicle and 30 GPS satellites.

Likewise, only at the time when the satellites are in view, the GPS simulator generates the range errors attributed to all error sources, which are depicted in Fig.9. In Fig.9, the increase of the receiver drift error along with simulation time incurs the explicit divergence of range errors. The geometric ranges plus corresponding range errors are the generated pseudorange measurements, which are given in Fig.10.

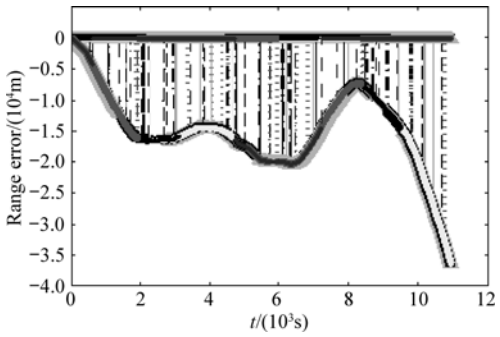

Fig.9 Range errors for pseudorange measurements.

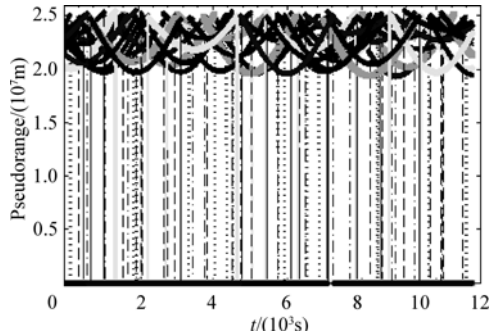

Fig.10 Simulated pseudorange measurements of 30 GPS satellites.

The integer ambiguity for each carrier phase measurement is given in Fig.11. Fig.12 presents the simulated carrier phase measurements on the basis of pseudorange measurements and the integer ambiguity.

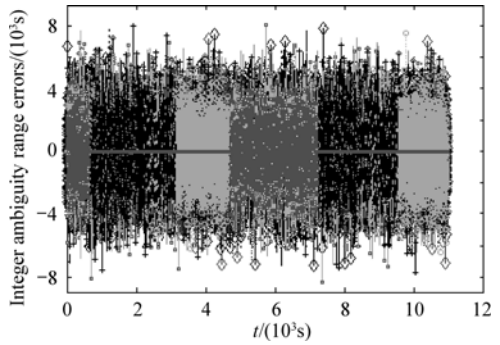

Fig.11 Integer ambiguity for each carrier phase measurement.

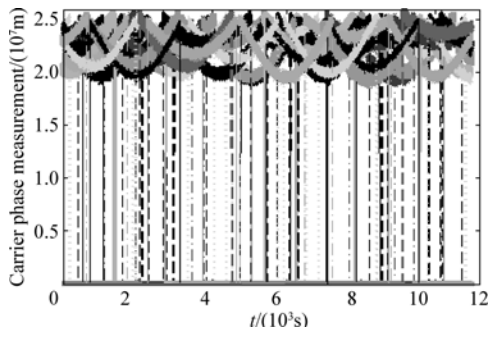

Fig.12 Simulated carrier phase measurements of 30 GPS satellites.

7. Conclusions

(1) This article addresses an enhanced high-fidelity simulator of GPS measurements, which is dedicated to promoting the design of a space-oriented GPS/INS integration system. Since the range rate is reckoned in the simulation procedure, the generated pseudorange and carrier phase measurements are fit for space-oriented applications or other high speed environments. Feasible models attributed to all related error sources, in particular, the space ionospheric model are proposed in the article to guarantee accurate simulation. Since the simulator can handle ephemeris data at any time, one can use it to evaluate the performance of navigation system with different time scale. Additionally, the simulation covers all satellites in the GPS constellation, no matter which is visible for the receiver or not. Thus the all-in-view navigation mode is readily verified.

(2) Along with the work presented here, effective multipath modes are needed to develop for specific applications. The effects on satellite visibility and receiver measurement noise due to signal to noise ratio are being laid emphases on in our current work. Furthermore, as a common research topic, accurate ionospheric delay model is also our care in the following project.

References

[1] Goodman J L. A GPS receiver upgrade for the space shuttle—rationale and considerations. The 40th AIAA/ASME/SAE/ASEE Joint Propulsion Conference and Exhibit. 2004; 1-11.

[2] Goodman J L. Application of GPS navigation to space flight. IEEE Aerospace Conference Proceedings. 2005; 1837-1852.

[3] Gaylor D E. Integrated GPS/INS navigation system design for autonomous spacecraft rendezvous. PhD thesis, Austin: The University of Texas at Austin, 2003.

[4] Advanced GPS hybrid simulation (AGHS). <http://www.navsys.com/Products/aghs.htm>. NAVSYS Corporation, 2007.

[5] NAVSTAR GPS satellite constellation simulator—model SCS 3500. <http://www.l-3com.com/products-services/productservice.aspx?type=ps&id=144>.L3 Communications Interstate Electronics Corporation, 2005.

[6] Positioning and navigation—space-based GNSS applications. <http://www.spirent.com/Positioning-and-Navigation/Space.aspx>. Spirent Communications, 2008.

[7] Montenbruck O, Gill E. Ionospheric correction for GPS tracking of LEO satellites. Journal of Navigation 2002; 55: 293-304.

[8] Ebinuma T. Precision spacecraft rendezvous using global positioning system: an integrated hardware approach. PhD thesis, Austin: The University of Texas at Austin, 2001.

[9] NAVSTAR GPS Joint Program Office. NAVSTAR GPS space segment/navigation user interfaces. Technical Report IS-GPS-200. ARINC Engineering Services, LLC, 2004.

[10] Misra P, Enge P. Global positioning system: signals, measurements, and performance. 1st edition. Lincoln, MA, USA: Ganga-Jamuna Press, 2004; 124-157.

[11] Axelrad P, Brown R G. GPS navigation algorithms. In:

Parkinson B W, Spilker J J, Axelrad P, et al., editors. Global Positioning System: Theory and Applications. Washington, DC: AIAA, 1996; 409-433.
[12] Brown R G, Hwang P Y C. Introduction to random signals and applied Kalman filtering. 3rd edition. New York: John Wiley & Sons, 1997.
[13] Gustavsson P. Development of a MATLAB based GPS constellation simulation for navigation algorithm developments. Master thesis, Luleå: Luleå University of Technology, 2005.
[14] Montenbruck O, Garcia-Fernandez M. Ionospheric path delay models for spaceborne GPS. DLR-GSOC TN 05-07, 2005.
[15] Zumberge J F, Bertiger W I. Ephemeris and clock navigation message accuracy. In: Parkinson B W, Spilker J J, Axelrad P, et al., editors. Global Positioning System: Theory and Applications. Washington, DC: AIAA, 1996; 585-599.
[16] Kaplan E D, Hegarty C J. Understanding GPS: principles and applications. 2nd edition. Washington, DC: Artech House, 2006.
[17] Taylor J, Barnes E. GPS current signal-in-space navigation performance. Proceedings of the ION 2005 National Technical Meeting. 2005; 385-393.
[18] Parkinson B W. GPS error analysis. In: Parkinson B W, Spilker J J, Axelrad P, et al., editors. Global Positioning System: Theory and Applications. Washington, DC: AIAA, 1996; 469-483.
[19] Spilker J J. Satellite constellation and geometric dilution of precision. In: Parkinson B W, Spilker J J, Axelrad P, et al., editors. Global Positioning System: Theory and Applications. Washington, DC: AIAA, 1996; 177-208.

Biography:

Wang Liduan Born in 1979, he is a Ph.D. candidate at Shanghai Jiao Tong University (SJTU) now. From 2006, he has been involved in the study and research of inertial navigation algorithms and GPS/INS integration. At present, his interests focus on space-oriented navigation system design and deep integration technology, R&D of integrated MEMS IMU/GPS navigation system.
E-mail: lidwang@gmail.com

Appendix A

According to Eq.(10), the square of the geometric range can be expresed as

$$(\rho(t_R))^2 = (\boldsymbol{r}_S(t_S) - \boldsymbol{r}_R(t_R)) \cdot (\boldsymbol{r}_S(t_S) - \boldsymbol{r}_R(t_R)) \quad \text{(A1)}$$

with the transmission time t_S being a function of $\rho(t_R)$, i.e. $t_S = t_R - \rho(t_R)/c$, and $\mathrm{d}t_S/\mathrm{d}t_R = 1 - \dot{\rho}(t_R)/c$.

Differentiating both sides of Eq.(A1) with respect to t_R yields

$$\rho(t_R)\dot{\rho}(t_R) = (\boldsymbol{r}_S(t_S) - \boldsymbol{r}_R(t_R)) \cdot \left(\dot{\boldsymbol{r}}_S(t_S)\frac{\mathrm{d}t_S}{\mathrm{d}t_R} - \dot{\boldsymbol{r}}_R(t_R)\right) = (\boldsymbol{r}_S(t_S) - \boldsymbol{r}_R(t_R)) \cdot \left[\dot{\boldsymbol{r}}_S(t_S)\left(1 - \frac{\dot{\rho}(t_R)}{c}\right) - \dot{\boldsymbol{r}}_R(t_R)\right] \quad \text{(A2)}$$

Rearranging Eq.(A2), we obtain

$$\rho(t_R)\dot{\rho}(t_R) + (\boldsymbol{r}_S(t_S) - \boldsymbol{r}_R(t_R)) \cdot \left(\dot{\boldsymbol{r}}_S(t_S)\frac{\dot{\rho}(t_R)}{c}\right) = (\boldsymbol{r}_S(t_S) - \boldsymbol{r}_R(t_R)) \cdot (\dot{\boldsymbol{r}}_S(t_S) - \dot{\boldsymbol{r}}_R(t_R)) \quad \text{(A3)}$$

then the range rate is given as Eq.(11):

$$\dot{\rho}(t_R) = \frac{(\boldsymbol{r}_R(t_R) - \boldsymbol{r}_S(t_S)) \cdot (\dot{\boldsymbol{r}}_R(t_R) - \dot{\boldsymbol{r}}_S(t_S))}{\rho(t_R) - (\boldsymbol{r}_R(t_R) - \boldsymbol{r}_S(t_S)) \cdot (\dot{\boldsymbol{r}}_S(t_S)/c)} \quad \text{(A4)}$$

The LOS vector from the receiver to the jth GPS satellite $\boldsymbol{\rho}_j$ is defined as

$$\boldsymbol{\rho}_j = \boldsymbol{r}_{Sj}(t_S) - \boldsymbol{r}_R(t_R) \quad \text{(A5)}$$

differentiating both sides of Eq.(A5), we will get the following expression

$$\dot{\boldsymbol{\rho}}_j = \dot{\boldsymbol{r}}_{Sj}(t_S) - \dot{\boldsymbol{r}}_R(t_R) \quad \text{(A6)}$$

The expression can be equivalently written as

$$\boldsymbol{v}_{REL,j} = \boldsymbol{v}_{Sj}(t_S) - \boldsymbol{v}_R(t_R) \quad \text{(A7)}$$

where $\boldsymbol{v}_{REL,j}$ is the relative velocity between the receiver and the jth GPS satellite as defined formerly. From Eq.(A4), Eq.(A5) and Eq.(A7), the instantaneous range rate of the jth GPS satellite is formulated as follows:

$$\dot{\rho}_j(t_R) = \frac{\boldsymbol{\rho}_j \cdot \boldsymbol{v}_{REL,j}}{\rho_j(t_R) + \boldsymbol{\rho}_j \cdot (\boldsymbol{v}_{Sj}(t_S)/c)} \quad \text{(A8)}$$